

## Improvement of $\gamma$ -ray energy resolution of $\text{LaBr}_3:\text{Ce}^{3+}$ scintillation detectors by $\text{Sr}^{2+}$ and $\text{Ca}^{2+}$ co-doping

M. S. Alekhin,<sup>1</sup> J. T. M. de Haas,<sup>1</sup> I. V. Khodyuk,<sup>1</sup> K. W. Krämer,<sup>2</sup> P. R. Menge,<sup>3</sup> V. Ouspenski,<sup>4</sup> and P. Dorenbos<sup>1</sup>

<sup>1</sup>*Department of Radiation Science and Technology, Faculty of Applied Sciences, Delft University of Technology, Mekelweg 15, 2629 JB Delft, The Netherlands*

<sup>2</sup>*Department of Chemistry and Biochemistry, University of Bern, Freiestrasse 3, 3012 Bern, Switzerland*

<sup>3</sup>*Saint-Gobain Crystals, 17900 Great Lakes Parkway, Hiram, Ohio 44234, USA*

<sup>4</sup>*Saint Gobain Recherche, 39, Quai Lucien Lefranc, 93303 Aubervilliers, France*

(Received 14 March 2013; accepted 14 April 2013; published online 26 April 2013)

Commercially available  $\text{LaBr}_3:5\% \text{Ce}^{3+}$  scintillators show with photomultiplier tube readout about 2.7% energy resolution for the detection of 662 keV  $\gamma$ -rays. Here we will show that by co-doping  $\text{LaBr}_3:\text{Ce}^{3+}$  with  $\text{Sr}^{2+}$  or  $\text{Ca}^{2+}$  the resolution is improved to 2.0%. Such an improvement is attributed to a strong reduction of the scintillation light losses that are due to radiationless recombination of free electrons and holes during the earliest stages (1–10 ps) inside the high free charge carrier density parts of the ionization track. © 2013 AIP Publishing LLC. [<http://dx.doi.org/10.1063/1.4803440>]

Scintillating materials have been applied for more than a century,<sup>1</sup> and they played a crucial role in the discovery of X-rays,  $\beta$ -particles, and  $\alpha$ -particles and today in the quest for the Higgs boson. Not long after the development of the photomultiplier tube (PMT) around 1940, the very important  $\text{NaI}:\text{Tl}^+$  scintillation crystal was discovered.<sup>2</sup> Till today  $\text{NaI}:\text{Tl}$  accounts for 80% of all scintillator volume sold world-wide.  $\text{Lu}_2\text{SiO}_5:\text{Ce}^{3+}$  (LSO:Ce) combines a strong interaction with  $\gamma$ -rays because of its high density and the presence of the high atomic number Lu atoms, with a very fast scintillation decay time of 35 ns from the lanthanide  $\text{Ce}^{3+}$ . It makes this material ideally suited for medical imaging in positron emission tomography (PET)-scanners.<sup>3</sup> Modern day PET-scanners may contain tens of thousands of individual  $2 \times 2 \times 20 \text{ mm}^3$  LSO:Ce crystal pixels to generate a three dimensional image of a scanned patient.<sup>4</sup> The electromagnetic calorimeter at CERN, Geneva, which is used for the quest for the Higgs boson, contains 110 000 23 cm long  $\text{PbWO}_4$  scintillating crystals<sup>5</sup> developed in the 1990s. Starting from the year 2000, we developed the  $\text{Ce}^{3+}$  activated La-halide scintillators, first  $\text{LaCl}_3:\text{Ce}$  (Ref. 6) and later  $\text{LaBr}_3:\text{Ce}$ .<sup>7</sup> Particularly  $\text{LaBr}_3:\text{Ce}$  combines excellent properties, i.e., an extremely fast scintillation pulse (16 ns) and a record low energy resolution for the detection of  $\gamma$ -rays. A full width at half maximum (FWHM) resolution of 2.8% at 662 keV was unequalled at that time.

In this letter we present a study on  $\text{Sr}^{2+}$  and  $\text{Ca}^{2+}$  co-doped  $\text{LaBr}_3:5\% \text{Ce}^{3+}$  and  $\text{CeBr}_3$  scintillators. We will show that such co-doping improves the linearity of scintillation response with X-ray or  $\gamma$ -ray energy. As a result, the energy resolution improves, and record of low energy resolutions of 2.0% at 662 keV and 6.5% at 59.5  $\gamma$ -ray detection will be demonstrated. One set of  $\text{Ca}^{2+}$  and  $\text{Sr}^{2+}$  co-doped samples used in this study were grown by the University of Bern. The starting materials  $\text{LaBr}_3$ ,  $\text{CeBr}_3$ ,  $\text{SrBr}_2$ , and  $\text{CaBr}_2$  were obtained from oxides with the  $\text{NH}_4\text{Br}$  method. To avoid moistening, the starting materials and products were always handled and stored in a  $\text{N}_2$  glove box. The starting materials were weighted in the corresponding stoichiometric ratios

(total of 8 g) into silica ampoules and sealed under high vacuum. 5 mol. % of  $\text{CeBr}_3$  and 0.5 mol. % of either  $\text{SrBr}_2$  or  $\text{CaBr}_2$  were added. The mixtures were molten in a horizontal tube furnace and homogenized. The ampoules were placed in vertical Bridgman furnaces, heated to approximately  $10^\circ\text{C}$  above their melting points and then cooled to RT over a period of 14 days. Another independent set of  $\text{Sr}^{2+}$  co-doped samples were provided by the Saint-Gobain Company. They were synthesized with a propriety method also used for the commercially available BriLanCe380 standard  $\text{LaBr}_3:5\% \text{Ce}$  scintillators. The  $\text{Ce}^{3+}$  concentration added to the starting material was 5 mol. %, and 0.35 mol. %–0.75 mol. % of  $\text{SrBr}_2$  was added. An ICP (Inductively Coupled Plasma) analysis on the samples revealed that typically 200 ppm of  $\text{Sr}^{2+}$  is actually incorporated in the final single crystal.

Small samples of about  $3 \times 3 \times 1 \text{ mm}^3$  size were cut from the original larger single crystal boule and mounted on top of the entrance window of a standard bialkali Hamamatsu R1791 PMT or a super bialkali Hamamatsu R6231-100 PMT. The sample was covered with several layers of white reflecting Teflon tape to ensure optimal photon collection on the PMT window. Scintillation pulse height spectra of  $^{137}\text{Cs}$  and  $^{241}\text{Am}$  radioactive sources were recorded with conventional techniques using an electronic shaping time of  $10 \mu\text{s}$ . Since the samples are hygroscopic all experiments were performed in an M-Braun UNILAB dry box with moisture content less than 1 ppm. The scintillation yield, or number of detected photons by the PMT, was obtained from the ratio of the scintillation charge output pulse and the charge output pulse generated by the detection of one single photon as outlined in Refs. 8 and 9. The method and equipment used for avalanche photodiode (APD) readout was the same as reported in Ref. 8. An electronic shaping time of  $2 \mu\text{s}$  was used. Scintillator response studies were also performed at the X1 X-ray station of Hasylab in Hamburg, Germany. In these studies the sample was sealed in a silica ampoule and mounted on a PMT placed directly in front of the output slit of a tunable double Bragg reflection monochromator providing an X-ray resolution of 1 eV at 9 keV rising to 20 eV at 100 keV. A  $50 \times 50 \mu\text{m}$  slit

area was used assuring that always the same small volume of the sample was irradiated.

One may distinguish three contributions to the energy resolution  $R$ , and assuming that they are independent from one another

$$R^2 = \frac{2.35^2}{N_{ndp}} + R_{intr}^2 + R_{det}^2 \quad (1)$$

applies. The first term is from the Poisson statistics in the number of detected photons  $N_{ndp}$ , the second term is an intrinsic contribution from the scintillator. The third term contains the contributions from variations in crystal quality throughout the bulk, variations in photon collection efficiency on the entrance window of the photon detector, and a noise contribution from the photon detector. By means of proper crystal growth and packaging technology this contribution needs to be minimized. Figure 1 shows the energy resolution  $R$  at 662 keV as observed for current day scintillators that are readout with an ordinary bialkali PMT against the fundamental limit  $R_{ndp} \equiv 2.35/\sqrt{N_{dph}}$ . The best resolution of 2.65% is observed for  $\text{LaBr}_3:\text{Ce}$ . Only  $\text{SrI}_2:\text{Eu}$  approaches similar energy resolution<sup>10,11</sup> when small samples are used.

Scintillator research always aimed to increase  $N_{ndp}$  in order to minimize  $R_{ndp}$ . Such strategy directed research towards smaller bandgap materials; first chlorides, then bromides, and nowadays the iodides are intensively investigated.<sup>10,12</sup> The importance of the intrinsic contribution has always been neglected in scintillation research and development, probably because its true physical origin was not clear and also not measurable. Yet, the large deviation between  $R$  and  $R_{ndp}$  for the widely applied  $\text{LSO}:\text{Ce}$ ,  $\text{NaI}:\text{Tl}$ , and  $\text{CsI}:\text{Tl}$  scintillators in Fig. 1 must be attributed to such intrinsic contribution. It is caused by a scintillator response that is not proportional to the amount of ionization energy deposited in the scintillator.<sup>13,14</sup> Figure 2 compares the response curves

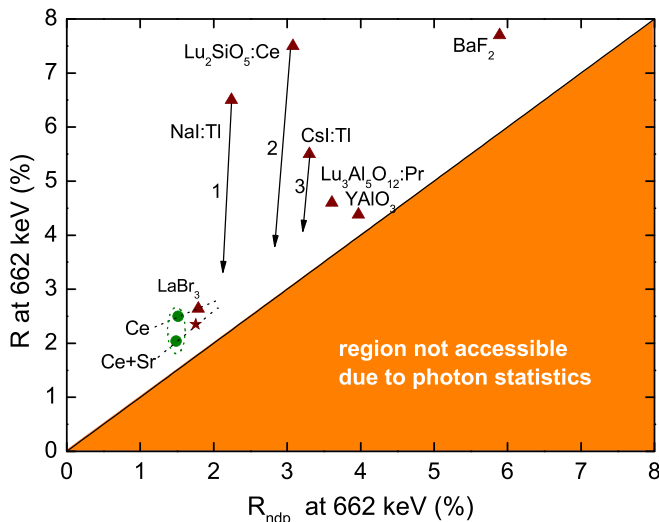


FIG. 1. The energy resolution of common scintillators at 662 keV energy with ordinary bialkali PMT readout against the contribution  $R_{ndp}$  from photon statistics. The encircled two data points are with a Hamamatsu super bialkali R6231-100 PMT. Arrows 1, 2, and 3 indicate potential improvements.  $\blacktriangle$  Data are from Ref. 14. The other data are from this work.

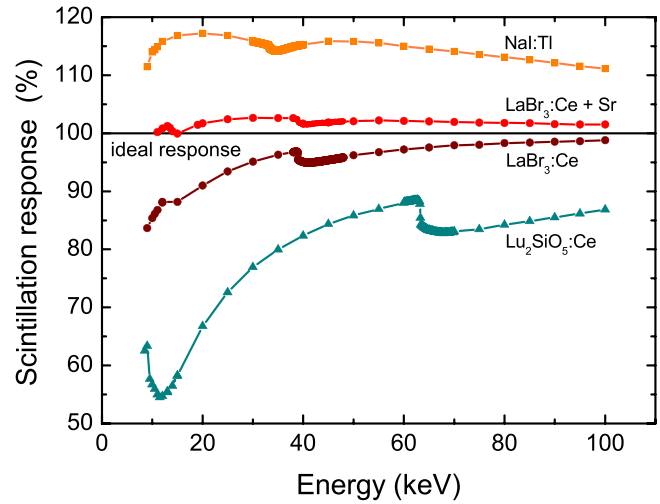


FIG. 2. The X-ray response curves for the scintillators  $\text{NaI}:\text{Tl}^+$ ,  $\text{Lu}_2\text{SiO}_5:\text{Ce}^{3+}$ ,  $\text{LaBr}_3:5\%\text{Ce}^{3+}$ , and  $\text{LaBr}_3:5\%\text{Ce}^{3+}$  co-doped with  $\text{Sr}^{2+}$ . All curves are normalized to 100% at 662 keV energy.

for  $\text{NaI}:\text{Tl}$ ,<sup>15</sup>  $\text{Lu}_2\text{SiO}_5:\text{Ce}$ ,<sup>16</sup> and  $\text{LaBr}_3:5\% \text{Ce}$  (Ref. 17) as has been determined with monochromatic synchrotron X-ray excitation. Here the scintillation response is defined as the ratio of the photon yield/MeV observed at the X-ray energy set by the monochromator to the photon yield/MeV observed at 662 keV, and ideally it is 100% at all energies. The response of  $\text{NaI}:\text{Tl}$  at 20 keV is 17% higher than at the reference energy of 662 keV, whereas  $\text{LSO}:\text{Ce}$  is almost 35% less efficient.  $\text{LaBr}_3:5\% \text{Ce}$  approaches best the ideal response, and indeed it shows the lowest energy resolution in Fig. 1. Recently we found that the shape of the response curve of  $\text{LaBr}_3:\text{Ce}$  depends on the temperature<sup>17</sup> and the  $\text{Ce}^{3+}$  concentration,<sup>18</sup> which demonstrates that the shape is not a truly fundamental property of a scintillator and that it can be altered.

A main cause for non-ideal response at low X-ray energy is radiationless electron-hole pair recombination that takes place in the high ionization density parts of the ionization track. That means close ( $<5 \text{ nm}$ ) to the track, and since the energy loss  $dE/dx$  of the ionizing primary electron increases with decreasing electron velocity (or energy  $E$ ), the recombination losses are highest at the end of the main track.<sup>19</sup> It is also high in the side tracks of secondary electrons created by “head-on collisions” of the primary electron with electrons of the scintillating medium. The stochastic nature of side track formation is the origin of  $R_{intr}$ . Only when the scintillation yield is independent on the electron energy,  $R_{intr}$  will vanish and the fundamental limiting energy resolution  $R_{ndp}$  comes within reach.

With the idea in mind that the shape of the response curve can be altered we decided to study the effect of  $\text{Sr}^{2+}$  and  $\text{Ca}^{2+}$  co-dopants on the performance of standard  $\text{LaBr}_3:5\% \text{Ce}$  scintillators. In Fig. 2 the response curve for a  $\text{Sr}^{2+}$  co-doped  $\text{LaBr}_3:5\% \text{Ce}$  scintillator has been added. A large improvement as compared to standard commercial  $\text{LaBr}_3:5\% \text{Ce}$  scintillators is observed, and the response is much closer to the ideal one.<sup>20</sup> The samples grown at the University of Bern and those at Saint-Gobain showed similar response curves. We also studied the response curve for  $\text{CeBr}_3$  which appears poorer than that of standard

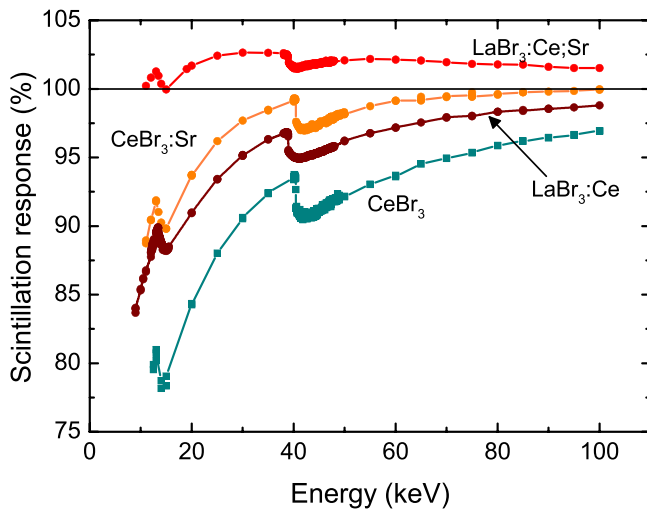


FIG. 3. The response curves for  $\text{CeBr}_3$  and  $\text{Sr}^{2+}$  codoped  $\text{CeBr}_3$  scintillators compared with that of a standard  $\text{LaBr}_3:5\%\text{Ce}$  scintillator.

$\text{LaBr}_3:5\%\text{Ce}$  as shown in Fig. 3. This is consistent with an observed poorer energy resolution of about 3.8% at 662 keV. Like in  $\text{LaBr}_3:5\%\text{Ce}$ , co-doping with  $\text{Sr}^{2+}$  improves the response curve of  $\text{CeBr}_3$  significantly. It is not yet as ideal as in  $\text{LaBr}_3:\text{Ce},\text{Sr}$ , but we expect that by changing the co-doping concentration or by using different type of co-dopants the response can be further engineered towards the ideal one.

The improved response in the 10–100 keV region has consequences for the light yield and energy resolution at 662 keV. With a standard bialkali PMT, about 17 200 photons are detected from a standard  $\text{LaBr}_3:5\%\text{Ce}$  scintillation crystal at 662 keV  $\gamma$ -ray energy. By using a Hamamatsu R6231-100 super bialkali PMT or a cooled APD that are higher quantum efficiency photon detectors  $N_{dph}$  increases to 24 000 and to 42 700, respectively. Resolution improves from 2.7% to 2.5% and to 2.45%. With Eq. (1) one then obtains  $R_{intr} \approx 1.9\%$ , and evidently  $R_{intr}$  provides the dominant contribution to the observed resolution. The star data symbol in Fig. 1 shows that the energy resolution with a standard bialkali PMT for a Sr co-doped sample improves to 2.35%. With the super bialkali PMT the improvement is more impressive as shown with the  $^{137}\text{Cs}$  source pulse height spectrum in Fig. 4. The total absorption peak at 662 keV shows a record low resolution of 2.0%. The peak due to 33 keV  $\text{La-K}_\alpha$  X-ray fluorescence escape is fully separated from the main peak, and also the  $\text{Ba-K}_\alpha$  and  $\text{Ba-K}_\beta$  X-ray fluorescence from the  $^{137}\text{Cs}$  source can be very well distinguished (see the inset of Fig. 4). We now calculate that for the Sr co-doped scintillator  $R_{intr}$  has lowered to  $\approx 1.3\%$  which is clearly connected with the more ideal response curve in Fig. 2. We predict that with well cooled APD readout, when  $R_{det}$  becomes insignificant, a resolution of 1.8% should be feasible. First tests at 8 °C gave 2.0% energy resolution, and improvements are to be expected with further cooling.

Fig. 5 compares the pulse height spectrum of a  $^{241}\text{Am}$  source measured with a standard and a Sr-co-doped  $\text{LaBr}_3$  scintillation crystal. Resolution at 59.5 keV improves from 9.4% to 6.5%. Also, the peaks between 10 and 30 keV are much better resolved in the Sr co-doped sample.

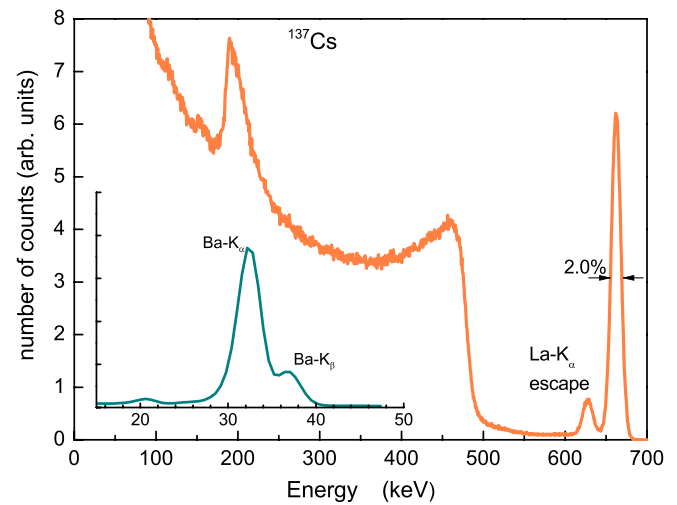


FIG. 4. Pulse height spectrum of a  $^{137}\text{Cs}$  source measured with a  $\text{Sr}^{2+}$  codoped  $\text{LaBr}_3:5\%\text{Ce}$  crystal and a Hamamatsu R6231-100 super bialkali PMT. The inset shows the 10–50 keV region on a reduced vertical scale.

Figures 2 and 3 show a strong drop in the response curves when passing the K-shell or sometimes L-shell electron binding energies of the atoms in the scintillator material. The drop at the threshold is caused by a re-distribution of the available X-ray energy over a set of secondary electrons with relatively low energy that each creates ionization tracks. A better representation of the response of a scintillator is obtained by measuring the response as function of electron energy instead of as function of X-ray or  $\gamma$ -ray energy. We recently developed a method to obtain such a response down to very low electron energy of 100 eV.<sup>16</sup> By tuning the X-ray energy just above the K-shell electron binding energy  $E_K$  of the most heavy element in the scintillator, a K-shell photoelectron will be ejected. The energy of this electron can be controlled within 10 eV accuracy simply by tuning the X-ray energy. One thus creates an internal electron source that is tunable from 100 eV to, say, 60 keV. The excess scintillation light produced by that photoelectron can be derived from the

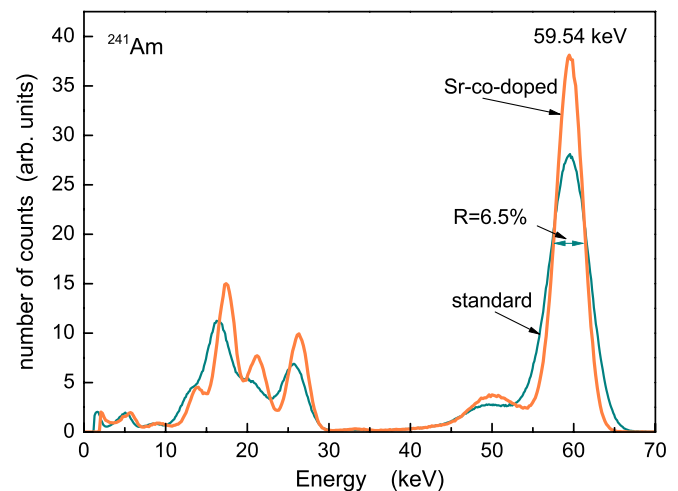


FIG. 5. Pulse height spectrum of an  $^{241}\text{Am}$  source measured with a standard  $\text{LaBr}_3:5\%\text{Ce}$  and a  $\text{Sr}^{2+}$  co-doped  $\text{LaBr}_3:5\%\text{Ce}$  scintillator on a Hamamatsu R6231-100 super bialkali PMT. Spectra are normalized such that the integral number of counts are the same. The peak at 59.54 keV was used for energy calibration assuming an ideal proportional response.

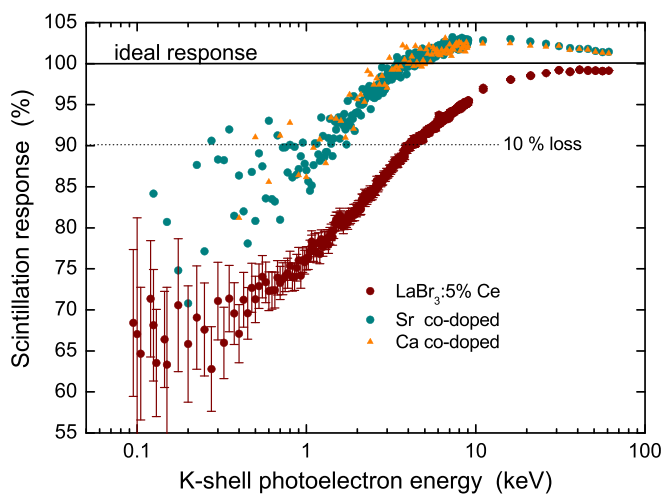


FIG. 6. The K-shell photo-electron response curves for standard  $\text{LaBr}_3:5\% \text{Ce}$  and  $\text{Sr}^{2+}$  and  $\text{Ca}^{2+}$  co-doped samples.

data. With this so-called K-dip spectroscopy method, response curves as a function of K-shell photoelectron energy were obtained as shown in Fig. 6. It reveals that  $\text{Ca}^{2+}$  and  $\text{Sr}^{2+}$  co-doping alter the response curve of standard  $\text{LaBr}_3:5\% \text{Ce}$  in a similar fashion. The point of 10% recombination loss is at 4.1 keV in the standard  $\text{LaBr}_3:5\% \text{Ce}$  scintillator, and it shifts towards 1.3 keV in the  $\text{Sr}^{2+}$  and  $\text{Ca}^{2+}$  co-doped scintillators. Since energy loss  $-dE/dx$  of a track creating electron increases with  $\approx 1/E$ ,<sup>21</sup> this implies that the ionization density at 1.3 keV is three times higher than at 4.1 keV. Apparently, the scintillator has become a factor of three more tolerant towards high ionization density recombination losses by the co-doping with either  $\text{Sr}^{2+}$  or  $\text{Ca}^{2+}$ .

The charge carrier dynamics taking place on the nm length scale around the track and in the ps time scale are extremely complicated<sup>19,22</sup> and at this stage not fully understood. The current idea is that the nonradiative recombination rate  $\Gamma_{nr}$  of free electrons and holes competes with the trapping rate  $\Gamma_{tr}$  of those charge carriers by  $\text{Ce}^{3+}$ . Once trapped by Ce the desired radiative recombination will follow.  $\Gamma_{nr}$  increases with ionization density, and it is therefore highest at the end points of the main and side tracks. When carrier mobility is high the free charge carriers may escape from the high ionization density parts of the track to survive the quenching phase, and one may define an escape rate  $\Gamma_{esc}$ . Since temperature affects the carrier mobility and  $\text{Ce}^{3+}$  concentration affects the carrier trapping rate,<sup>18</sup> the co-doping either reduces  $\Gamma_{nr}$  or increases  $\Gamma_{esc}$  or  $\Gamma_{tr}$  in order to explain the improved proportionality.

In conclusion, we demonstrated that the response curve of  $\text{LaBr}_3:5\% \text{Ce}$  scintillators can be improved by  $\text{Sr}^{2+}$  co-doping. The intrinsic resolution  $R_{intr}$  at 662 keV is then reduced from 1.9% to 1.3% which results in 2.0% energy resolution when scintillation readout is done by a super bialkali

PMT. We anticipate that a resolution of 1.8% should be possible with well cooled APD read-out. We found that  $\text{Ca}^{2+}$  co-doping has similar effect as  $\text{Sr}^{2+}$  co-doping, and both coponents also improve the response curve of  $\text{CeBr}_3$  scintillators. The implications of the improved energy resolution of  $\text{LaBr}_3:5\% \text{Ce}$  are immediate. Particularly for applications where energy resolution is crucial, e.g., in nuclear isotope identifiers, the benefits of co-doping are evident. With a better resolution, different isotopes are more reliably detected which is of particular importance in systems for homeland security inspections and for nuclear non-proliferation.

This work was funded by the Dutch Technology Foundation (STW) and supported by Saint-Gobain Crystals, France and by the European Community's Seventh Framework Program (FP7/2007-2013) under Grant Agreement No. 226716. We sincerely thank Dr. A. Owens and Dr. F. Quarati for sharing their beamtime at the synchrotron with us and their assistance in some of the experiments.

- <sup>1</sup>M. J. Weber, *J. Lumin.* **100**, 35 (2002).
- <sup>2</sup>R. Hofstadter, *Phys. Rev.* **74**, 100 (1948).
- <sup>3</sup>C. L. Melcher, *J. Nucl. Med.* **41**, 1051 (2000).
- <sup>4</sup>P. Zanzonico, *Semin. Nucl. Med.* **XXXIV**(2), 87 (2004).
- <sup>5</sup>S. Chatrchyan, G. Hmayakyan, and V. Khachatryan *et al.*, *J. Instrum.* **3**, S08004 (2008).
- <sup>6</sup>E. V. D. van Loef, P. Dorenbos, C. W. E. van Eijk, K. Krämer, and H. U. Güdel, *Appl. Phys. Lett.* **77**, 1467 (2000).
- <sup>7</sup>E. V. D. van Loef, P. Dorenbos, C. W. E. van Eijk, K. Krämer, and H. U. Güdel, *Appl. Phys. Lett.* **79**, 1573 (2001).
- <sup>8</sup>J. T. M. de Haas and P. Dorenbos, *IEEE Trans. Nucl. Sci.* **55**, 1086 (2008).
- <sup>9</sup>M. Bertolaccini, S. Cova, and C. Bussolati, in Proceedings of International Symposium on Nuclear Electronics, Versailles, France, 10–13 September 1968, pp. 8-1.
- <sup>10</sup>N. J. Cherepy, G. Hull, A. D. Drobshoff, S. A. Payne, E. van Loef, C. M. Wilson, K. S. Shah, U. N. Roy, A. Burger, L. A. Boatner, W.-S. Choong, and W. W. Moses, *Appl. Phys. Lett.* **92**, 083508 (2008).
- <sup>11</sup>M. S. Alekhin, J. T. M. de Haas, K. W. Krämer, and P. Dorenbos, *IEEE Trans. Nucl. Sci.* **58**, 2519 (2011).
- <sup>12</sup>E. D. Bourret-Courchesne, G. Bizarri, R. Borade, Z. Yan, S. M. Hanrahan, G. Gundiah, A. Chaudhry, A. Canning, and S. E. Derenzo, *Nucl. Instrum. Methods Phys. Res. A* **612**, 138 (2009).
- <sup>13</sup>P. Dorenbos, J. T. M. de Haas, and C. W. E. van Eijk, *IEEE Trans. Nucl. Sci.* **42**, 2190 (1995).
- <sup>14</sup>P. Dorenbos, *IEEE Trans. Nucl. Sci.* **57**, 1162 (2010).
- <sup>15</sup>I. V. Khodyuk, P. A. Rodnyi, and P. Dorenbos, *J. Appl. Phys.* **107**, 113513 (2010).
- <sup>16</sup>I. V. Khodyuk, J. T. M. de Haas, and P. Dorenbos, *IEEE Trans. Nucl. Sci.* **57**, 1175 (2010).
- <sup>17</sup>I. V. Khodyuk, M. S. Alekhin, J. T. M. de Haas, and P. Dorenbos, *Nucl. Instrum. Methods Phys. Res. A* **642**, 75 (2011).
- <sup>18</sup>I. V. Khodyuk, F. G. A. Quarati, M. S. Alekhin, and P. Dorenbos, "Charge carrier mobility and related energy resolution of  $\text{LaBr}_3:\text{Ce}$  scintillators" (unpublished).
- <sup>19</sup>R. T. Williams, J. Q. Grim, Q. Li, K. B. Ucer, and W. W. Moses, *Phys. Status Solidi B* **248**, 426 (2011).
- <sup>20</sup>U.S. patent application 61/493,805 (6 June 2011).
- <sup>21</sup>G. F. Knoll, *Radiation Detection and Measurement* (John Wiley & Sons, Inc., New York, 1999).
- <sup>22</sup>A. Kozorezov, J. K. Wigmore, and A. Owens, *J. Appl. Phys.* **112**, 053709 (2012).